Quality evaluation of phase reconstruction in LED-based digital holography

Yi Qin (秦 怡)[1] and Jingang Zhong (钟金钢)[1,2*]

[1]*Department of Optoelectronic Engineering, Jinan University, Guangzhou 510632, China*

[2]*Key Laboratory of Optoelectronic Information and Sensing Technologies of Guangdong Higher Educational Institutes, Jinan University, Guangzhou 510632, China*

[*]*E-mail: tzjg@jnu.edu.cn*

Received July 15, 2009

An approach, based on the correlation between the intensity distribution of object wave of the directly recorded by charge-coupled device and the one reconstructed by computer, is proposed to evaluate the quality of the phase reconstruction in light emitting diode (LED) based phase-shifting digital holography. This method enables us to find out the optimal reconstructed phase even though the peak wavelength of LED, which is used for calibrating the phase-shifter, is inconvenient to be determined and tends to shift with temperature and driving current. The feasibility of this method is verified by both computer simulations and experiments.

OCIS codes: 090.1995, 120.5050, 110.3000.

doi: 10.3788/COL20090712.1146.

Digital holography is an increasingly attractive method for optical metrology[1,2]. It enables direct access to reconstruct both an intensity image and a phase image simultaneously[3]. The phase image can provide quantitative information about the three-dimensional (3D) structure of the specimen, which is one of the significant advantages of digital holography. How to acquire a high-quality phase image by numerical reconstruction has been a very important research topic. There are various factors that limit the quality of the phase image such as experimental setup, numerical reconstruction method, reconstruction parameter, etc. In many cases, whether the numerically reconstructed phase is equal to the true phase of the object wave is unknown. The quality of the phase reconstruction is usually evaluated by a standard sample. However, it would cause the invalidation of the evaluation under the following circumstances. 1) There are some inevitable accidental errors in the experiment, such as the accidental errors[4] introduced by the phase-shifter in the phase-shifting digital holography. 2) Due to the limitation of the reconstruction algorithm, the reconstruction process may be affected by the sample. For example, for the numerical reconstruction methods including the angular spectrum method and the Fresnel diffraction integral method, in order to filter out the zero-order term, the twin image term, and the parasitic interferences, the process of spatial filtering must be carried out. Different spatial filters should be made according to the distribution of the spectrum that varies with different samples[5].

Light emitting diode (LED) sources open up prospects for noise reduction in digital holography by suppression of speckle noises and parasitic interferences in the experimental setup[6−9]. Due to LED's short coherence length, the digital holography based on LED is confined to phase-shifting digital holography[8−10]. Generally speaking, the peak wavelength of the LED should be known to calibrate the phase-shifter. However, it is always inconvenient to determine the peak wavelength because each LED has a different peak wavelength although they might share the same model and manufacturer, and the peak wavelength tends to shift with temperature and driving current[11]. Therefore, the calibration of the phase-shifter becomes difficult. Moreover, the nonlinear error of the phase-shifter is inevitable[12]. Therefore, it would cause the invalidation of the evaluation which employs the standard sample to evaluate the quality of the phase reconstruction for LED-based digital holography. To resolve these problems, in this letter, an approach for evaluating the quality of the phase reconstruction by investigating the correlation between the intensity distribution of object wave directly recorded by a charge-coupled device (CCD) and that reconstructed by a computer rather than through the use of standard samples is proposed. The method enables us to find out the optimal reconstructed phase in LED-based phase-shifting digital holography. The use of correlation to determine the errors from the ideal reconstruction to real reconstruction in quadrature phase-shifting holography has recently been used by Liu *et al.*[13]

A typical setup for LED-based phase-shifting digital

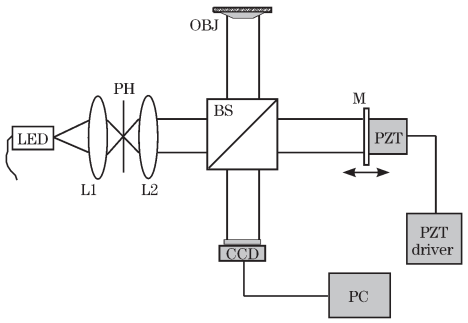

Fig. 1. Modified Michelson interferometer for phase-shifting digital holography. L1, L2: lenses; PH: pinhole; OBJ: object measured; BS: beam splitter; M: mirror; PC: personal computer; PZT: piezoelectric transducer.

holography is shown in Fig. 1. A set of LEDs illuminate a modified Michelson interferometer. The LED beam is converged by a lens L1 to the pinhole (PH) and transformed to a parallel beam by another lens L2. The parallel beam is separated into two beams by a beam splitter (BS). One beam serves as a reference wave, and the other illuminates the object to be measured (OBJ). The reference wave is reflected by a mirror M attached on a piezoelectric transducer (PZT) that is used for phase-shifting. The BS combines the object wave and reference wave, and the holograms are recorded by a CCD camera.

The discussion will concentrate on the four-step phase-shifting holography for simplicity. The intensity distribution $I_i(x,y)$ recorded by the CCD can be written as

$$\begin{aligned} I_i(x,y) =& I_{\mathrm{R}}(x,y) + I_{\mathrm{O}}(x,y) \\ &+2\sqrt{I_{\mathrm{O}}(x,y)I_{\mathrm{R}}(x,y)}\cos[\phi(x,y)+\varphi_i], \\ &(i=1,\ 2,\ 3,\ 4), \end{aligned} \tag{1}$$

where (x,y) are the coordinates of the hologram plane; $\varphi_i = (i-1)\pi/2$ is the phase shift introduced by moving the reference mirror by quarter wavelength intervals; $\phi(x,y)$ is the relative phase between the object wave and the reference wave on the hologram plane; $I_{\mathrm{O}}(x,y)$ and $I_{\mathrm{R}}(x,y)$ are the intensity distributions of the object wave and reference wave on the hologram plane, respectively. In principle, the complex amplitude distribution of the object wave on the hologram plane can be reconstructed by

$$\begin{aligned} O_{\mathrm{d}}(x,y) =& \frac{1}{4\sqrt{I_{\mathrm{R}}(x,y)}}\{[I_1(x,y)-I_3(x,y)] \\ &+ \mathrm{i}[I_4(x,y)-I_2(x,y)]\}. \end{aligned} \tag{2}$$

The reconstructed phase of the object wave is

$$\phi_{\mathrm{d}}(x,y) = \tan^{-1}\left[\frac{I_4(x,y)-I_2(x,y)}{I_1(x,y)-I_3(x,y)}\right]. \tag{3}$$

The reconstructed intensity of the object wave is

$$\begin{aligned} I_{\mathrm{d}}(x,y) &= |O_{\mathrm{d}}(x,y)|^2 \\ &= \frac{1}{16I_{\mathrm{R}}(x,y)}\{[I_1(x,y)-I_3(x,y)]^2 \\ &\quad + [I_4(x,y)-I_2(x,y)]^2\}. \end{aligned} \tag{4}$$

When there is no phase-shifting error, it can be concluded that

$$\begin{cases} I_{\mathrm{d}}(x,y) = I_{\mathrm{O}}(x,y) \\ \phi_{\mathrm{d}}(x,y) = \phi(x,y) \end{cases}. \tag{5}$$

Assuming that α_1, α_2, and α_3 are the first, second, and third step phase-shifting errors generated by PZT, the four images recorded by CCD can be expressed as

$$\begin{cases} I_1(x,y) = I_{\mathrm{R}}(x,y) + I_{\mathrm{O}}(x,y) + 2\sqrt{I_{\mathrm{O}}(x,y)I_{\mathrm{R}}(x,y)}\cos[\phi(x,y)] \\ I_2(x,y) = I_{\mathrm{R}}(x,y) + I_{\mathrm{O}}(x,y) + 2\sqrt{I_{\mathrm{O}}(x,y)I_{\mathrm{R}}(x,y)}\cos[\phi+\frac{\pi}{2}+\alpha_1] \\ I_3(x,y) = I_{\mathrm{R}}(x,y) + I_{\mathrm{O}}(x,y) + 2\sqrt{I_{\mathrm{O}}(x,y)I_{\mathrm{R}}(x,y)}\cos[\phi(x,y)+\pi+\alpha_2] \\ I_4(x,y) = I_{\mathrm{R}}(x,y) + I_{\mathrm{O}}(x,y) + 2\sqrt{I_{\mathrm{O}}(x,y)I_{\mathrm{R}}(x,y)}\cos[\phi(x,y)+\frac{3\pi}{2}+\alpha_3] \end{cases}. \tag{6}$$

The reconstructed intensity obtained by Eq. (4) can be written as

$$\begin{aligned} I_{\mathrm{d}}(x,y) =& \frac{1}{16I_{\mathrm{R}}(x,y)}\{[I_1(x,y)-I_3(x,y)]^2 \\ &+[I_4(x,y)-I_2(x,y)]^2\} \\ =& \frac{1}{4}I_{\mathrm{O}}(x,y)\{[\cos(\phi(x,y))+\cos(\phi(x,y)+\alpha_2)]^2 \\ &+[\sin(\phi(x,y)+\alpha_1)+\sin(\phi(x,y)+\alpha_3)]^2\}. \end{aligned} \tag{7}$$

The reconstructed phase obtained by Eq. (3) can be written as

$$\begin{aligned} &\phi_{\mathrm{d}}(x,y) \\ &= \tan^{-1}\left\{\frac{\sin[\phi(x,y)+\alpha_3]+\sin[\phi(x,y)+\alpha_1]}{\cos\phi(x,y)+\cos[\phi(x,y)+\alpha_2]}\right\}. \end{aligned} \tag{8}$$

Comparing Eq. (5) with Eqs. (7) and (8), it is obvious that phase-shifting errors α_1, α_2, and α_3 lead to the differences between $I_{\mathrm{d}}(x,y)$ and $I_{\mathrm{O}}(x,y)$, $\phi_{\mathrm{d}}(x,y)$ and $\phi(x,y)$. Therefore, we can evaluate the similarity between the reconstructed phase $\phi_{\mathrm{d}}(x,y)$ and the true phase $\phi(x,y)$ of the object wave by investigating the similarity between the reconstructed intensity $I_{\mathrm{d}}(x,y)$ and the true intensity $I_{\mathrm{O}}(x,y)$ of the object wave which is recorded directly by the CCD on the hologram plane. The more similar $I_{\mathrm{d}}(x,y)$ and $I_{\mathrm{O}}(x,y)$, the more similar $\phi_{\mathrm{d}}(x,y)$ and $\phi(x,y)$. The correlation coefficient between $I_{\mathrm{d}}(x,y)$ and $I_{\mathrm{O}}(x,y)$ can be employed to evaluate the similarity of them. The correlation coefficient between matrices A and B is given by[14]

$$\rho_{AB} = \frac{\mathrm{COV}(A,B)}{\sqrt{D_A D_B}}, \tag{9}$$

where COV(A,B) is the covariance of A and B, D_A and D_B are the variances of A and B, respectively. For matrices A and B with the sizes of mxn, there is

$$\begin{cases} D_A = \dfrac{1}{mn}\sum\limits_{i=1}^{m}\sum\limits_{j=1}^{n}(A_{ij}-\overline{A})^2 \\ D_B = \dfrac{1}{mn}\sum\limits_{i=1}^{m}\sum\limits_{j=1}^{n}(B_{ij}-\overline{B})^2 \\ \mathrm{COV}(A,B) = \dfrac{1}{mn}\sum\limits_{i=1}^{m}\sum\limits_{j=1}^{n}(A_{ij}-\overline{A})(B_{ij}-\overline{B}) \end{cases}, \tag{10}$$

where A_{ij} and B_{ij} are elements of matrices A and B, $\overline{A} = \dfrac{1}{mn}\sum\limits_{i}^{m}\sum\limits_{j}^{n}A_{ij}$ and $\overline{B} = \dfrac{1}{mn}\sum\limits_{i}^{m}\sum\limits_{j}^{n}B_{ij}$. The range of ρ_{AB} is $1 \geq \rho_{AB} \geq -1$.

So the correlation coefficient between $I_{\mathrm{d}}(x,y)$ and

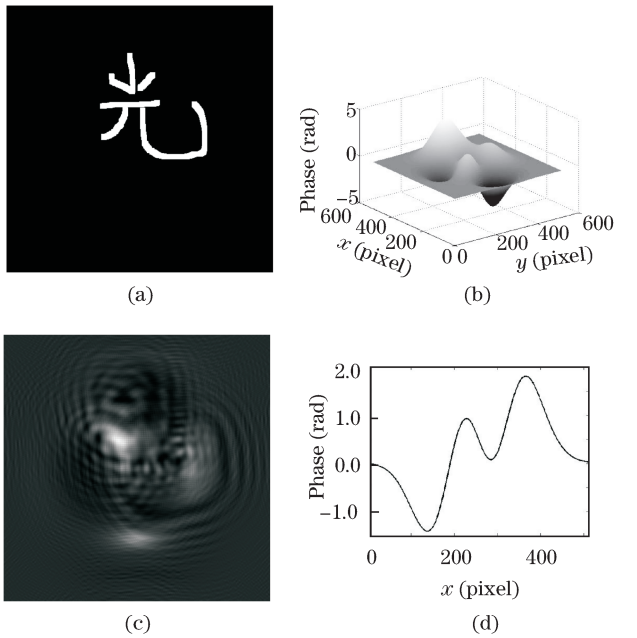

Fig. 2. Simulated object. (a) The amplitude and (b) the phase distributions of the object. (c) The intensity of the object wave on hologram plane recorded by the CCD. (d) The phase distribution at the 256th row.

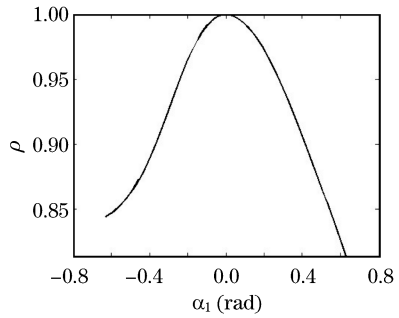

Fig. 3. Relationship between ρ and α_1.

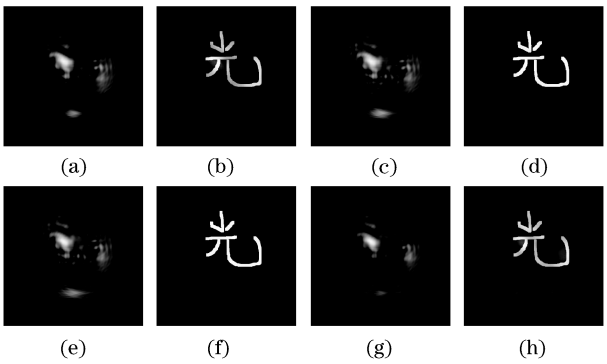

Fig. 4. Reconstructed intensity images. (a), (c), (e), (g) on the hologram plane and (b), (d), (f), (h) on the object plane with $\alpha_1 = \pi/10$, $\rho = 0.9380$; $\alpha_1 = \pi/50$, $\rho = 0.9970$; $\alpha_1 = -\pi/50$, $\rho = 0.9967$; $\alpha_1 = -\pi/10$, $\rho = 0.9205$, respectively.

$I_{\rm O}(x, y)$ can be expressed as

$$\rho = \frac{\mathrm{COV}(I_d, I_{\rm O})}{\sqrt{D_{I_{\rm d}} D_{I_{\rm o}}}}. \tag{11}$$

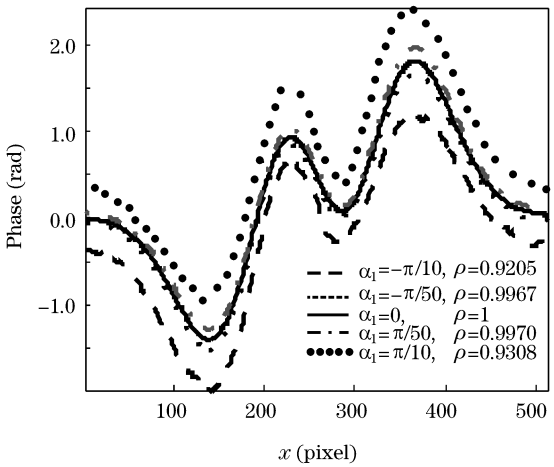

Fig. 5. Reconstructed phase distributions of the object with different phase-shifting errors at the 256th row.

The higher the absolute value of the correlation coefficient ρ, the more similar $I_{\rm d}(x, y)$ and $I_{\rm O}(x, y)$, i.e., the more similar $\phi_{\rm d}(x, y)$ and $\phi(x, y)$. Therefore, the correlation coefficient ρ can be employed to achieve real-time evaluation of the reconstructed phase, where $I_{\rm d}(x, y)$ can be reconstructed by Eq. (4) and $I_{\rm O}(x, y)$ is recorded by the CCD after removing the reference beam in the setup as shown in Fig. 1.

A computer simulation is performed to demonstrate the validity of the evaluation method based on the correlation coefficient of $I_{\rm d}(x, y)$ and $I_{\rm O}(x, y)$. The apparatus employed in the simulation is illustrated in Fig. 1. Figure 2(a) and (b) show the amplitude and phase distributions of the simulated object with the size of 512×512 pixels. The intensity of the object wave $I_{\rm O}(x, y)$ on the hologram plane is shown in Fig. 2(c). The propagation distance between object plane and CCD plane is $d = 300$ mm. Figure 2(d) shows the phase distributions of the simulated object at the 256th row.

For simplicity, if the PZT has a good linearity and the PZT driver is of sufficient resolution, it can be concluded that

$$\begin{cases} \alpha_2 = 2\alpha_1 \\ \alpha_3 = 3\alpha_1 \end{cases}. \tag{12}$$

That is, the phase-shifting error will be transferred step-by-step, and each step has the same linear error due to the inaccurate voltage exerted on the PZT. Thereby, Eqs. (7) and (8) can be simplified to

$$I_{\rm d}(x, y) = \frac{1}{4} I_{\rm O}(x, y)\{[\cos(\phi(x, y)) + \cos(\phi(x, y) + 2\alpha_1)]^2 + [\sin(\phi(x, y) + \alpha_1) + \sin(\phi(x, y) + 3\alpha_1)]^2\}, \tag{13}$$

$$\phi_{\rm d}(x, y) = \tan^{-1}\left\{\frac{\sin[\phi(x, y) + 3\alpha_1] + \sin[\phi(x, y) + \alpha_1]}{\cos\phi(x, y) + \cos[\phi(x, y) + 2\alpha_1]}\right\}. \tag{14}$$

This means that $I_{\rm d}(x, y)$ will just rely on α_1. For phase-shifting error, it can be expected that $\alpha_1 \ll \frac{\pi}{2}$. A

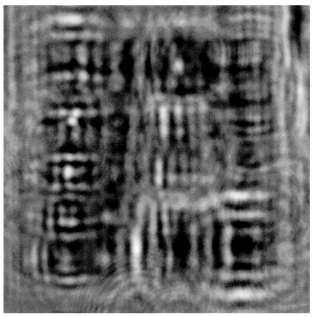

Fig. 6. Intensity image of object wave on the hologram plane recorded by the CCD.

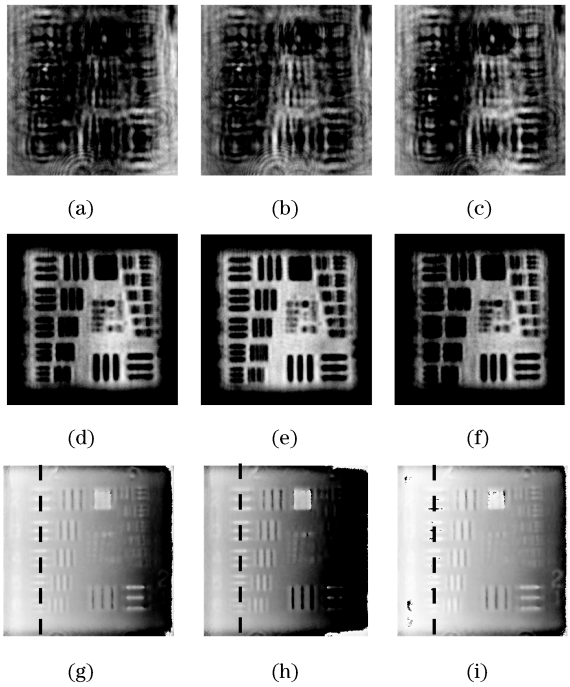

Fig. 7. Reconstructed intensity and phase distributions with different phase-shifting voltages. (a)−(c)The reconstructed intensity distributions on the hologram plane, (d)−(f) the reconstructed intensity distributions, and (g)−(i) the wrapped phase distributions on the object plane with U = 6.0 V, ρ = 0.8194; U = 6.6 V, ρ = 0.8700; U = 7.2 V, ρ = 0.8233, respectively.

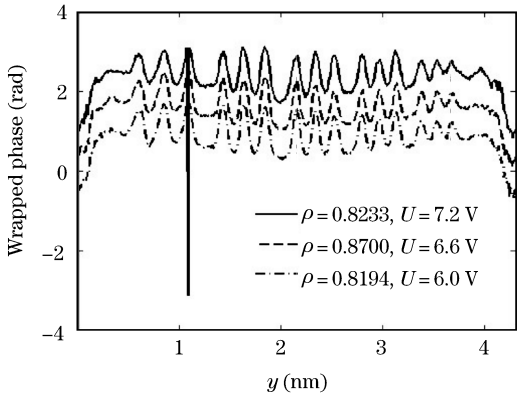

Fig. 8. Phase distributions at the cross sections marked with dashed lines in Figs. 7(g), (h), and (i).

reasonable inference can be made that the similarity between $I_{\rm d}(x,y)$ and $I_{\rm O}(x,y)$ will decline with the increase of the absolute value of α_1.

Figure 3 shows the relationship between ρ and α_1, where the value of α_1 varies from $-\pi/5$ to $\pi/5$ with the interval of $\pi/200$, and for each α_1 there is a corresponding ρ calculated according to Eqs. (11) and (13). It shows evidently that the value of ρ decreases with the increase of the absolute value of α_1, and the maximum ρ appears at $\alpha_1 = 0$. Therefore, the value of ρ can be considered as a good index that reveals the phase-shifting error.

Figure 4 shows the reconstructed intensity images with different phase-shifting errors. Figure 4(a), (c), (e), and (g) show the reconstructed intensity images on the hologram plane with phase-shifting errors $\alpha_1 = \pi/10$, $\pi/50$, $-\pi/50$, and $-\pi/10$, i.e., ρ = 0.9380, 0.9970, 0.9967, and and 0.9205, respectively. Figures 4(b), (d), (f), and (h) show the corresponding reconstructed intensity images on the object plane with the mentioned phase-shifting error, respectively. The corresponding reconstructed phase distributions on the object plane are shown in Fig. 5. From Figs. 4(b), (d), (f), and (h), it can be seen that the quality of reconstructed intensity image decreases as the value of ρ decreases. Figure 5 shows that the deviation of the reconstructed phase distributions from the true phase distribution increases with the decrease of the value of ρ. The results indicate that the quality of the reconstructed object wave depends on the value of ρ which is determined by α_1. Therefore, the value of ρ can be employed as a criterion to evaluate the quality of the reconstructed object wave.

The experimental setup is shown in Fig. 1. The measured object was Resolution Values for Standard USAF 1951 Resolution Test Pattern. The aperture of pinhole PH is 108 μm. An ultra-bright red LED was used. Holograms were recorded by the CCD camera (Mintron 22K9HC, 795×596 pixels, 8.33×8.33 μm^2 per pixel) with 8-bit gray scale output. The PZT phase-shifter was calibrated by a He-Ne laser (λ = 632.8 nm) with 6.3-V driving voltage, leading to a $\pi/2$ phase shift.

Figure 6 shows the intensity image of the object wave recorded by the CCD camera with the reference beam being turned off. Different driving voltages were employed to obtain different phase-shifting errors. For each voltage value U, four holograms were obtained by driving PZT at 0, U, $2U$, and $3U$. The intensity images and phase images can be reconstructed by Eqs. (4) and (3), respectively. The correlation coefficient ρ can be obtained by Eq. (11). Figure 7 shows the reconstructed images. Figures 7(a), (b), and (c) are the reconstructed intensity images on the hologram plane with driving voltages U = 6.0, 6.6, and 7.2 V. Figures 7(d), (e), and (f) are the reconstructed intensity images on the object plane, respectively. Figures 7(g), (h), and (i) are the reconstructed wrapped phase images on the object plane. The phase distributions at the cross sections marked with dashed lines in Fig. 7 are shown in Fig. 8. It is obvious that the reconstructed phase distributions with different driving voltages are different. Figure 9 shows the correlation coefficients with different voltages exerted on PZT for phase-shifting. It can be seen that ρ reaches its maximum of 0.87 at U = 6.6 V. It can be

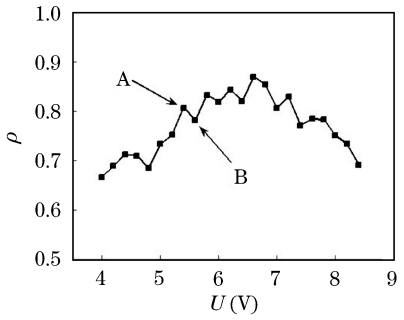

Fig. 9. Correlation coefficient ρ versus voltage U exerted on PZT for phase-shifting.

judged that phase-shifting error would be the smallest at $U = 6.6$ V and the reconstructed object wave would be the optimal. It can be observed that the values of ρ are fluctuant and not always consistent with the ideal curve shown in Fig. 3. Taking point A for example, normally, compared with point B, a larger phase-shifting error α_1 and a smaller ρ are expected according to Fig. 3. The nonlinearity of PZT, the shift of peak wavelength of LED, and the instability of experimental setup may be the causes of fluctuation[4,11,12]. In other words, the accidental errors of phase-shifter have arisen. Therefore, the phase-shifting error at point B may be greater than that at point A, and the quality of reconstructed object-wave at point A is better than that at point B.

In conclusion, both the computer simulations and the experimental results indicate that the correlation coefficient between the reconstructed intensity and the true intensity of the object wave reflects the quality of the reconstructed images. It means that the optimal reconstruction phase images can be determined according to the value of the correlation coefficient in phase-shifting digital holography, even though the accidental errors of phase-shifter have arisen and the calibration of phase-shifter has not been made. Therefore, a new method, by employing the correlation coefficient, for evaluation of the quality of the phase reconstruction and the phase-shifting error in phase-shifting digital holography, which is based on LED, is proposed. Furthermore, once the maximum of the correlation coefficient has been determined, it can be considered as a reference index for the latter phase-shifting holography experiments employing the same experimental apparatus. It makes one free from the troublesome calibration of PZT phase-shifter for digital holography based on LED.

This work was supported by the National Natural Science Foundation of China under Grant No. 60677019.

References

1. H. Wang, D. Wang, J. Zhao, and J. Xie, Chin. Opt. Lett. **6,** 165 (2008).
2. Z. Feng, F. Jia, J. Zhou, and M. Hu, Chinese J. Lasers (in Chinese) **35,** 2017 (2008).
3. E. Cuche, P. Marquet, and C. Depeursinge, Appl. Opt. **38,** 6994 (1999).
4. P. J. de Groot, J. Opt. Soc. Am. A **12,** 354 (1995).
5. J. Weng, J. Zhong, and C. Hu, Opt. Express **16,** 21971 (2008).
6. J. Maycock, B. M. Hennelly, J. B. McDonald, Y. Frauel, A. Castro, B. Javidi, and T. J. Naughton, J. Opt. Soc. Am. A **24,** 1617 (2007).
7. X. Kang, Chin. Opt. Lett. **6,** 100 (2008).
8. N. Warnasooriya and M. K. Kim, Opt. Express **15,** 9239 (2007).
9. B. Kemper, S. Stürwald, C. Remmersmann, P. Langehanenberg, and G. von Bally, Opt. Lasers Eng. **46,** 499 (2008).
10. I. Yamaguchi and T. Zhang, Opt. Lett. **22,** 1268 (1997).
11. M. Bürmen, F. Pernuš, and B. Likar, Meas. Sci. Technol. **19,** 122002 (2008).
12. Y.-Y. Cheng and J. C. Wyant, Appl. Opt. **24,** 3049 (1985).
13. J.-P. Liu and T.-C. Poon, Opt. Lett. **34,** 250 (2009).
14. R. C. Gonzalez and R. E. Woods, *Digital Image Processing* (Prentice Hall, New York, 2002).